

# Preparation, characterization and catalytic activity towards green reactions of sulfonic functionalized SBA-15

Elena I. Basaldella · M. Soledad Legnoverde ·  
Ignacio Jiménez-Morales ·  
Enrique Rodríguez-Castellón · Bruno O. Dalla Costa ·  
Carlos A. Querini

Received: 1 October 2010 / Accepted: 28 February 2011 / Published online: 18 March 2011  
© Springer Science+Business Media, LLC 2011

**Abstract** Acidic heterogeneous catalysts based on the anchorage of sulfonic groups on SBA-15 mesoporous silica were synthesized. In a first synthesis step, samples containing mercapto groups were prepared by co-condensation of tetraethylorthosilicate with 3-mercaptopropyltrimethoxysilane, in presence of ethylene-propylene block copolymer as mesoporous silica structure director. In other samples, mercapto groups were introduced by post-functionalization of the traditional calcined SBA-15. In a second step, these mercapto groups were oxidized in order to get sulfonic acid groups on the surface. Characterization of the samples was carried out by  $N_2$  adsorption-desorption, FTIR, XPS and acid-base titration. Spectroscopic techniques showed that the effective incorporation of sulfonic groups depends on the synthesis methodology used. In turn, the SBA-15 post-

synthesis functionalization produces changes in structural characteristics like a decrease in BET surface and changes in the pore size distribution. The as-prepared materials were tested as acid catalysts in the alkylation of isobutane with 1-butene, and in the esterification of free fatty acids with methanol. The results obtained show a lack of activity in the alkylation reaction which can be associated with the formation and stabilization of the intermediate carbocation species.

**Keywords** Mesoporous silica · SBA-15 · Functionalization · Sulfonation · Acid catalysts · Alkylation · Esterification

## 1 Introduction

Synthesis of chemical products of great industrial importance often leads to the use of mineral acids as homogeneous catalysts. This type of synthesis presents as main drawback, the generation of considerable amounts of toxic residues. Consequently, in recent years there has been developed a great interest in the study of organic transformations performed under heterogeneous catalysts, because of the possibility for recovering and recycling the solids, and therefore significantly reducing the environmental impact (Izumi et al. 1993; Moffat 2001; Kozhevnikov 2002 and Chakrabarti and Sharma 1993).

Industrial processes requiring electrophilic catalysts use corrosive and particularly hazardous materials such as sulfuric acid (Russell and Frye 1955),  $HClO_4$  (Bulut and Erk 1996),  $P_2O_5$  (Robertson et al. 1931) and aluminum chloride (Potdar et al. 2001). A wide range of acidic solids has been proposed to replace these aggressive materials.

E.I. Basaldella (✉) · M.S. Legnoverde  
Centro de Investigación y Desarrollo en Ciencias Aplicadas Dr.  
J.J. Ronco (CINDECA), Universidad Nacional de La Plata,  
CCT-La Plata CONICET, CIC, 47 No 257, 1900 La Plata,  
Argentina  
e-mail: [eib@quimica.unlp.edu.ar](mailto:eib@quimica.unlp.edu.ar)

E.I. Basaldella · M.S. Legnoverde  
Departamento de Ingeniería Química, Facultad Regional La Plata,  
Universidad Tecnológica Nacional, 124 y 60, 1900 La Plata,  
Argentina

I. Jiménez-Morales · E. Rodríguez-Castellón  
Departamento de Química Inorgánica, Unidad Asociada al  
Instituto de Catálisis (CSIC), Facultad de Ciencias, Universidad  
de Málaga, 29071 Málaga, Spain

B.O. Dalla Costa · C.A. Querini  
Instituto de Investigaciones en Catálisis y Petroquímica  
(INCAPE), CONICET, Facultad de Ingeniería Química,  
Universidad Nacional del Litoral, (UNL), Santiago del Estero  
2654, S3000AOJ, Santa Fe, Argentina

For example, molecular sieves (Izumi et al. 1993), heteropolyacids (Izumi et al. 1993; Moffat 2001; Kozhevnikov 2002) or resins containing sulfonic groups have already been used in industrial practices. However, these materials show some disadvantages, such as low thermal stability and hydrophilicity (Sharma 1995; Harmer and Sun 2001; Olah et al. 1985). In the particular case of the alkylation of isobutane with C<sub>4</sub> olefins, the usual catalysts used at industry are sulfuric acid and fluorhydric acid. Different zeolite-based catalysts have been studied in order to replace the homogeneous catalysts, but deactivation has been the limiting factor for their application at industrial level, being this deactivation mainly attributed to the micropore blockage (Querini et al. 1997, Querini and Roa 1997; Ginosar et al. 2004). Therefore, it seems that ordered mesoporous silicas or their functionalized derivatives might be a good alternative (Dalla Costa et al. 2009), since in this case the larger pore diameter might allow the product to diffuse out of the pores, thus decreasing the coke deposition rate.

Different mesoporous materials have been recently investigated in acid-catalyzed reactions. SBA-15 and periodic mesoporous organosilicas (PMO) materials have been investigated (Shen et al. 2008, 2010). These supports have been functionalized and used in different reactions. There are several options to design this type of catalysts. It is possible to select different alkyl groups, such as ethyl, propyl, butyl, and isobutyl, among others, in order to incorporate the functional group. In addition, the functional groups can also be varied, for example alkylsulfonic, arene sulfonic (Hamoudi and Kaliaguine 2003; Hamoudi et al. 2004), and perfluorinated sulfonic acid groups (Melero et al. 2006) have been used.

In this work, we used SBA-15 as support, since it has a better thermal stability than the PMO materials, in which the siloxane moieties are bridged by organic groups. However, the PMO materials are also very interesting materials since they are hydrophobic (Shen et al. 2008), and this is quite important as discussed by Shen et al. (2008), and as we suggest in the present study.

Surface modification of SBA-15 can be readily accomplished by all the methods developed for silica (Wight and Davis 2002; Ford et al. 2005; Lim and Stein 1999; Yoshitake 2005). For the synthesis of SBA-15 containing sulfonic groups, the usual procedure is carried out in two steps. In the first step, mercapto groups are attached to the pore surface. The introduction of this surface group can be done either during the sol-gel reaction of hexagonal arrangement of mesopores (co-condensation) or by post-synthesis functionalization. The mercapto group is then oxidized to sulfonic group (Bossaert et al. 1999). Nevertheless, some authors have attained the oxidation and grafting simultaneously (Margolles et al. 2000). Alternatively, it is also possible the attachment of sulfonic groups to the pre-bounded surface mercapto groups (Niknam et al. 2009).

In this work, we carried out some modifications to these different preparation methodologies, such as increasing reaction time or modification of the reaction temperature, in order to obtain a large number of acid sites with high acidity.

To assess the catalytic activity of the prepared materials, they were firstly tested in the alkylation of isobutane with 1-butene reaction. The adsorption/desorption processes were studied by transient experiments, in order to obtain information regarding the kinetics of these physical steps in the reaction mechanism. These experiments were also useful to learn about the interaction between the olefin and the surface of catalysts.

Additionally, the prepared catalysts were tested in the esterification of free fatty acids (FFA) with methanol (MeOH), and the activities results obtained for the two catalytic reactions are compared and discussed. This is an important objective of this work, in order to understand the behavior of this type of materials. The two reactions studied in this work, are currently carried out using liquid sulphuric acid as catalyst.

## 2 Experimental

### 2.1 Material synthesis

#### 2.1.1 Mesoporous catalysts

Three different methodologies were employed in order to obtain sulfonic groups on the surface of SBA-15 silica.

**2.1.1.1 Functionalization by thiol group during the synthesis and post-oxidation** The mesoporous material containing mercaptopropyl groups on its surface was prepared by co-condensation of tetraethylorthosilicate (TEOS) (Aldrich) and mercaptopropyltrimethoxysilane (MPTS) (Aldrich), in the presence of poly(ethyleneglycol)-block-poly(propylene-glycol)-block-poly(ethyleneglycol) (PE-PP-PE) (Aldrich) in HCl acid medium (Baker). The molar composition of each mixture for 4 g of copolymer was 0.0369 TEOS:0.0041 MPTS:0.24HCl:6.67H<sub>2</sub>O. The resultant solution was stirred for 20 h at 40 °C, after which the mixture was aged at 80 °C for 70 h under static conditions. The solid product was recovered by filtration and air-dried at room-temperature overnight. The template was removed from the as-synthesized material by washing with ethanol under reflux for 24 h. The product was labeled SBAsh1. After thiol functionalization, oxidation proceeds by soaking the resulting solid in an aqueous dissolution of hydrogen peroxide (H<sub>2</sub>O<sub>2</sub> 30 vol%), following the method described by Bossaert et al. (1999). To eliminate PE-PP-PE situated inside the pores, the solid was washed with ethanol, followed

**Table 1** Preparation methods for the different catalysts

Sample	Preparation method
SBAorig	SBA-15 obtained according to Zhao et al. 1998
SBAsh1	Functionalization by SH during the synthesis of SBA-15
SBAulf1	Oxidation of SBAsh1 with $H_2O_2$ (Method 1).
SBAulf2	Functionalization by SH and oxidation to sulfonic during the synthesis of SBA-15 (Method 2).
SBAsh2	Functionalization by SH post synthesis SBAorig
SBAulf3	SBAsh2 + chlorosulfonic acid to incorporate sulfonic groups (Method 3).

by filtration. The wet material was suspended (1 wt%) in 1 M  $H_2SO_4$  solution for 2 h. The powder was then dried for 2 h at 120 °C. This sample was labeled SBAulf1. It is well known that some PE-PP-PE could be still retained by the sulfonic samples after ethanol washing. However, we determined by DSC that this amount is very small (result not shown), and consequently the effect of this deposit on the catalyst activity can be neglected.

**2.1.1.2 Functionalization by the thiol group and oxidation to sulfonic group during the same step** The functionalized material was prepared following the sol-gel methodology described in Sect. 2.1.1.1, with the sole difference that the incorporation of the hydrogen peroxide, used to produce the oxidation, was conducted simultaneously with the MPTS. This sample was labeled SBAulf2 (Margolles et al. 2000).

**2.1.1.3 Post synthesis functionalization by thiol group followed by functionalization with sulfonic groups** Calcined SBA-15 silica (SBAorig), obtained according to Zhao et al. (1998), was refluxed in a solution of MPTS in toluene, under stirring in  $N_2$  atmosphere for 24 h. The obtained solid was labeled SBAsh2. To a magnetically stirred mixture of SBAsh2 (5 g) in  $CHCl_3$  (20 mL), chlorosulfonic acid (1.00 g, 9 mmol) was added dropwise at 0 °C over 2 h. After addition completion, the mixture was stirred for another 2 h and then filtered, the solid washed with methanol (30 mL) and dried at room temperature (Niknam et al. 2009). This sample was named SBAulf3.

Table 1 summarizes the different samples and the corresponding preparation methodologies employed.

### 2.1.2 Microporous catalysts

Microporous material was prepared from a commercial Y-zeolite (UOP Y54) with a Si/Al ratio 2.4. The sodium form was first ion exchanged with a 0.5 M  $La(NO_3)_3$  solution, adding 10 ml/g, working at reflux conditions during 4 h, and then drying at 100 °C. Finally, the solid was calcined at 550 °C during 2 h. This material was used in a second ion exchange with a 0.5 M  $NH_4NO_3$  solution, adding 22 ml/g

under the same conditions, finishing the preparation by drying and then calcining the solid. The catalyst obtained with this procedure was labeled Y-LCH.

### 2.2 Characterization

The catalysts were characterized by SEM, XPS, FTIR, adsorption-desorption of  $N_2$  (−196 °C), and the acidity was analyzed by titrating with *n*-butylamine. The particles size and morphology were determined using SEM, with a Philips 505 microscope.

The nitrogen adsorption-desorption isotherms were measured at the temperature of liquid nitrogen using a Micrometrics apparatus ASAP 2020. Before adsorption, samples were outgassed by heating at 100 °C in vacuum, with a pressure lower than  $3 \times 10^{-2}$  mm Hg during 12 h. The change in acidity due to functionalization was determined by potentiometric titration. A known mass of the solid to be analyzed was suspended in acetonitrile. The suspension was titrated using a 0.1 N solution of *n*-butylamine in acetonitrile at 0.05 mL/min. The electrode potential variation was recorded on a digital pH meter (Metrohm 794 Basic Titrino apparatus with a double junction electrode). The surface composition analyses were conducted by X-Ray photoelectron spectrometry (XPS), using a Physical Electronics PHI 5700 spectrometer with non-monochromatic Mg  $K\alpha$  radiation (300 W, 15 kV, 1253.6 eV) for the analysis of the core level signals of O 1s, Si 2p, S 2p and C 1s and with a multi-channel detector. Solids samples were introduced in a sample holder and degassed at high vacuum during 12 h. Spectra of powdered samples were recorded with the constant pass energy values at 29.35 eV, using a 720  $\mu$ m diameter analysis area. During data processing of the XPS spectra, binding energy values were referenced to the C 1s peak (284.8 eV) from the adventitious contamination layer. The PHI ACCESS ESCA-V6.0 F software package was used for acquisition and data analysis. A Shirley-type background was subtracted from the signals. Recorded spectra were always fitted using Gauss-Lorentz curves, in order to determine the binding energy of the different elements more accurately. The error in BE was estimated to be ca. 0.1 eV.

FTIR spectra were recorded on a Shimadzu FTIR-8300 instrument using KBr pressed powder discs. Each ground sample (0.5 mg) was mixed with 100 mg of spectroscopically pure dry KBr and pressed into disks before its spectrum was recorded.

### 2.3 Activity test

#### 2.3.1 Alkylation of isobutane

The alkylation reaction of isobutane with butene was carried out in a fixed-bed reactor in liquid phase at 80 °C and

30 kg/cm<sup>2</sup>. The isobutane/C4 olefins molar ratio was 15, and the olefin weight hourly spatial velocity WHSV = 1 h<sup>-1</sup>. Prior to reaction the catalysts were pretreated by heating in situ at 1.5 °C/min in N<sub>2</sub> flow, from room temperature up to 300 °C in the case of the Y-LCH catalyst, and up to 120 °C for the functionalized samples. After 1 h, the reactor was cooled to reaction temperature, and the liquid mixture was stabilized at the desired flow rate by-passing the reactor. Finally, the isobutane-olefins mixture was sent to the reactor.

Due to the fast deactivation of the catalysts in this reaction and the complexity of the reaction mixture, the reaction products were collected at different times in a heated multi-loop valve, and then analyzed by gas chromatography.

After the reaction, the catalysts were purged with N<sub>2</sub> at 80 °C for 1 h.

### 2.3.2 Esterification of free fatty acids

By this reaction, free fatty acids present in the high acidity raw materials used in the production of biodiesel, are transformed into esters, reducing the acidity of the material as a previous stage to the transesterification.

The experiments were conducted in a stainless steel batch reactor (Parr model 4842) provided with a temperature controller, pressure transducer and magnetic stirrer, monitoring the reaction conditions at 170 °C and 21 atm, during 2 h. The reactants, free fatty acids (FFA), commercial sunflower oil and methanol, were charged together with the catalyst, at room temperature. The FFA mixture was produced from tall oil, and had 96.5% acidity, provided by M.A. Liberman & CIA S.R.L.—Arizona Chemical. This tall oil was obtained as a by-product of the Kraft process of wood pulp manufacture. Anhydrous methanol was used with a molar ratio (MR) alcohol/FFA 3:1, the initial acidity in the mixture FFA/sunflower oil was A° = 40%, and the catalyst loading was 6 wt% referred to the FFA content.

To monitoring the reaction, small samples of the reacting mixture were taken at different times. Then, there were washed and centrifuged in order to eliminate the catalyst and the alcohol. The free fatty acid content was analyzed according to UNE-EN 14104 (2003). Acidity (A) is expressed as grams of oleic acid (OA) per 100 grams of mixture (M).

### 2.4 Dynamic analysis of the catalytic interaction with 1-butene

The dynamic of the olefin adsorption-desorption on each catalyst surface, was studied by sending consecutive pulses of 1-butene diluted in N<sub>2</sub> to the sample cell at different temperatures.

SBAsulf2 and SBAsulf3 samples were pretreated in N<sub>2</sub> at 120 °C during 1 h and then the temperature was stabilized at the desired value before starting the experiments. For these

materials, the first cycle of pulses was sent at 40 °C. After the temperature was stabilized, 20 pulses of 2% butene/N<sub>2</sub> were sent to the sample every 10 seconds, using N<sub>2</sub> as carrier gas. Then, when the FID signal was stabilized, the temperature was increased 10 °C up to 50 °C, and a new series of pulses was sent. The procedure was repeated increasing the temperature in 10 °C steps up to 80 °C. Then, series of pulses were carried out, but decreasing the temperature to 80 °C, 60 °C, 50 °C and 40 °C.

For these experiments, the Y-LCH zeolite was pretreated at 350 °C during 1 h in N<sub>2</sub> flow. In this case, the initial temperature was 60 °C, increasing in 10 °C steps up to 100 °C.

This experimental design provides information regarding the strength of the interaction between the olefin and the catalyst, and if it is reversible or not. In addition, the comparison of the results obtained at each temperature during the heating and the cooling treatment, provides information regarding the deactivation that the 1-butene remaining on the surface, produces on the adsorption capacity.

The results for each material are compared with those obtained when the pulses are sent with the empty cell (blank experiment).

This experiment also has the objective of developing a simple and fast analytical tool for screening catalysts for the reaction under study, using very small amounts of material and reactants.

## 3 Results and discussion

### 3.1 Characterization by XPS

Table 2 shows the atomic concentrations determined by XPS. Samples containing considerable amounts of carbon and sulfur were obtained with the three preparation procedures used in this study. Figure 1 shows XPS spectra of the S 2p signal that correspond to the samples obtained using the different preparation methodologies. According to these analyses, sulfur is found only as S<sup>2-</sup> in the samples containing only mercapto groups (samples SBAsulf1 and SBAsulf2), with a doublet S 2p<sub>3/2</sub> and S 2p<sub>1/2</sub>, where the S 2p<sub>3/2</sub> peak appears centered at 163.0 eV. In the oxidized samples (SBAsulf1, SBAsulf2 and SBAsulf3), sulfur is observed under two oxidation states: S<sup>6+</sup> and S<sup>2-</sup>, ascribed to the simultaneous presence of sulfonic (S 2p<sub>3/2</sub> at 168.5 eV) and mercapto (S 2p<sub>3/2</sub> at 163.2 eV) groups.

Table 3 shows the percentages of both types of sulfur (Smrc and Ssulf). The results obtained using the first and second synthesis procedures, indicate that a complete oxidation of the mercapto groups is not achieved, though the oxidized percentage is higher when the second methodology is used. In the case of the third preparation method, the catalyst also contains both groups. Since no further oxidation step was performed, the fraction corresponding to the

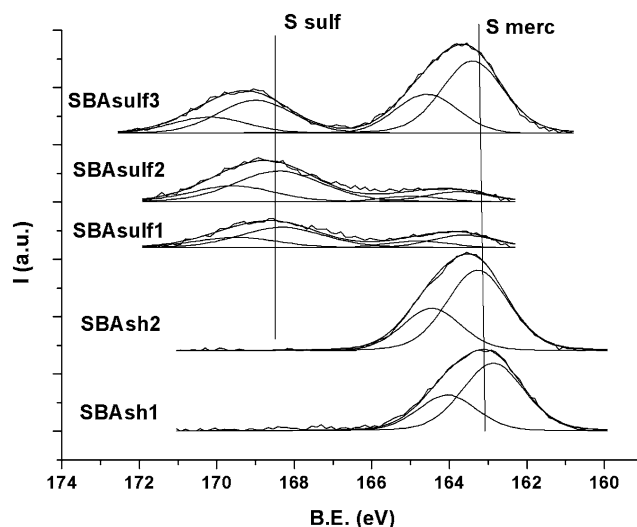


**Fig. 1** Core level S 2p spectra for the studied samples

**Table 2** Surface chemical composition (atomic concentration %) determined by XPS

Sample	%C	%O	%Si	%S
SBAorig	1.65	65.41	32.94	–
SBAsh1	23.57	50.72	23.62	2.09
SBAsulf1	14.08	56.34	27.84	1.40
SBAsulf2	10.70	59.71	27.42	1.61
SBAsulf3	16.85	54.54	26.33	2.28
	15.67	55.10	25.91	3.32

**Table 3** Percentage distribution of sulfur in mercapto groups and sulfonic groups

Sample	%S <sub>total</sub>	%S <sub>merc</sub>	%S <sub>sulf</sub>	S 2p <sub>3/2</sub> (eV)
SBAsh1	2.09	100	–	162.8
SBAsulf1	1.40	34	66	163.7
				168.7
SBAsulf2	1.61	23	77	163.8
				168.6
SBAsh2	2.28	100	–	163.1
SBAsulf3	3.32	67	33	163.2
				168.7

sulfonic group is much lower in this case, even though with this procedure it is possible to obtain a higher incorporation of sulfur. However, we must keep in mind that these results correspond to the surface of the samples and that the situation inside the pores may be different to that observed on the external surface.

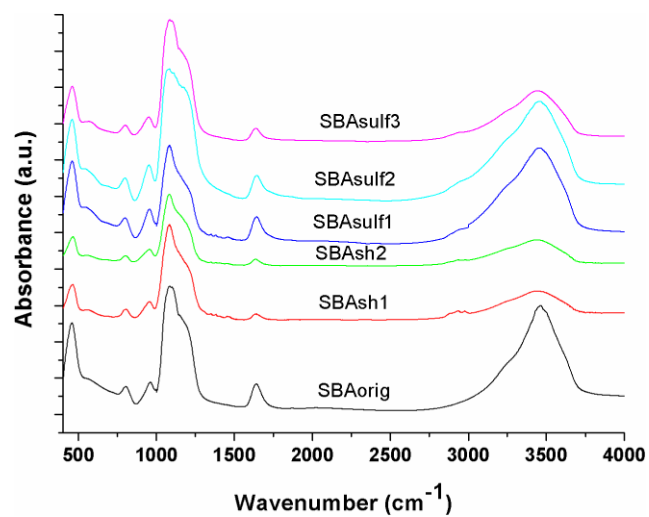


**Fig. 2** FTIR spectra corresponding to the original SBA-15, and to the functionalized and oxidized samples

### 3.2 FTIR analysis

The FTIR analysis shows variations in the spectra caused by the organo-functionalization. Figure 2 shows the spectra corresponding to the original sample (SBAorig) and to the samples after functionalization. The absorption band in the region between 3740 and 3000 cm<sup>-1</sup> is attributed to silanols groups, and the signal that appears at 2937 cm<sup>-1</sup> is assigned to the C–H bond stretching (Phan and Jones 2006; Li et al. 2006). The large absorbance reduction in the O–H region observed in the functionalized samples corroborates the substitution of the O–H groups by mercapto groups (Yang and Huang 2005). Signals at 460 and 800 cm<sup>-1</sup> and at 1080 and 1220 cm<sup>-1</sup> are associated to the torsion, symmetric stretching and asymmetric stretching of the Si–O bond, respectively.

Signals at 460 and 800 cm<sup>-1</sup> and at 1080 and 1220 cm<sup>-1</sup> are associated to the torsion, symmetric stretching and asymmetric stretching of the Si–O bond, respectively. It can be noticed that in the spectra corresponding to samples containing sulfonic groups, the Si–O stretching band at 1220 cm<sup>-1</sup> broadens towards higher wavenumbers and increases in intensity, due to the S=O stretching vibration mode associated to absorption bands observed at 1201 and 1121 cm<sup>-1</sup>.

### 3.3 Textural characterization

Figure 3a shows the N<sub>2</sub> adsorption–desorption isotherms that correspond to the different samples studied in this work. The isotherms are typical of type IV with a clear H1-type hysteresis loop at a high relative pressure (Sing et al. 1985).

The relationship between the adsorption increase at  $P/P_0 < 0.4$  corresponding to the multilayer adsorption and

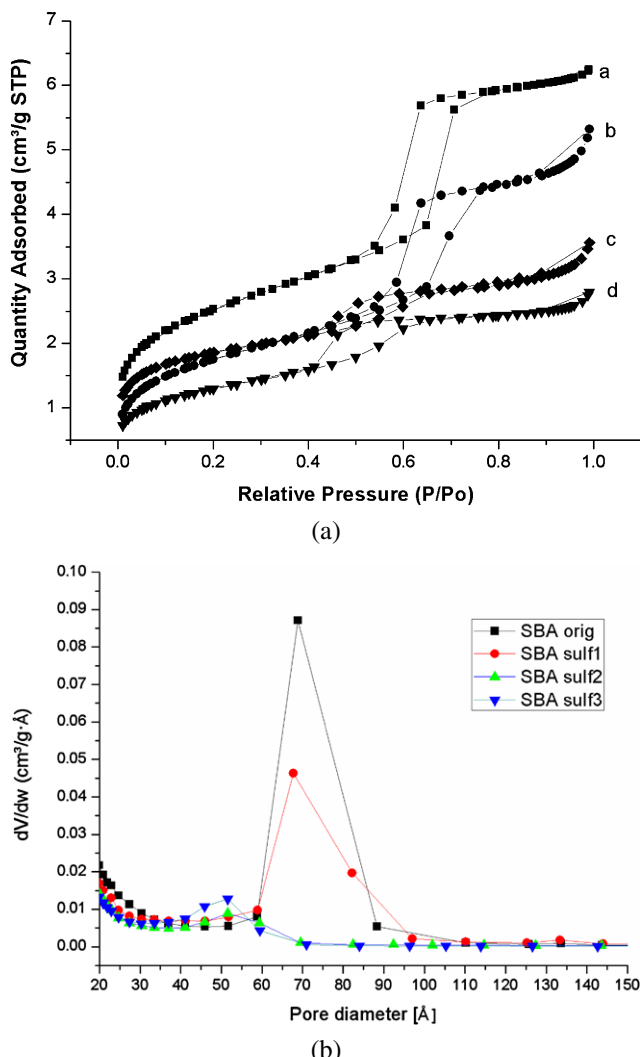


**Fig. 3** Textural analyses of prepared samples. (a) Adsorption-desorption nitrogen curves at  $-196^{\circ}\text{C}$ . (a) SBAorig, (b) SBAsulf1, (c) SBAsulf2, (d) SBAsulf3; (b) Pore size distributions

the second increase at  $P/P_0 = 0.4\text{--}0.7$ , depends on the presence of sulfonic groups. Additionally, functionalization produces changes in the hysteresis loop. The capillary condensation step, which corresponds to capillary condensation in cylindrical pores, occurred at lower pressure values for functionalized samples. A sharp adsorption step in the range of relative pressures  $P/P_0 = 0.55\text{--}0.77$  was registered for SBA-15orig and SBAsulf1, meanwhile SBAsulf2 and SBAsulf3 show hysteresis loops with moderate sharpness. The maximum displacement for the capillary condensation step was observed for the sample SBAsulf3, at  $P/P_0 = 0.42\text{--}0.55$ .

Table 4 shows the textural properties of the studied samples. BET areas are between 464 and 904 m<sup>2</sup>/g. A decrease in the BET area after post-functionalization can be observed.

The mesopore size distributions (Fig. 3b) were calculated using the thermodynamic-based Barret-Joyner-Halenda

**Table 4** Properties of sulfonic samples

Sample	BET (m <sup>2</sup> /g)	Pore Vol at $P/P_0 = 0.99$ (cm <sup>3</sup> /g)	Pore size (Å)	Acid sites density (μmol/m <sup>2</sup> )
SBAorig	904	0.962	70	–
sulf1	631	0.802	68	0.51
sulf2	662	0.536	53	0.59
sulf3	670	0.424	52	0.46

(BJH) method. The desorption branch of the isotherm was used for SBA-15orig and SBAsulf1. SBAsulf2 and SBAsulf3 appear to be spherical pore mesoporous materials because they exhibit the phenomenon of percolation in the desorption branch (because the hysteresis loop closes at  $P/P_0 \sim 0.42$ ). Hence, for these two samples the adsorption branch was used to evaluate their pore size distributions. A small reduction of the pore size and a noticeable diminution of the pore volume were obtained for functionalized samples (Table 4, columns 3 and 4).

Besides, SEM images (not shown) reveal the typical form of SBA-15 as agglomerates with the form of wheat grains composed of small cylinders. In the functionalized samples, the size of these agglomerates is smaller. SEM micrographs indicate that the presence of MPTS in the synthesis media do not alter the usual morphology presented by SBA-15 structure. Our results show that the addition of MPTS should be very carefully controlled (time, quantity) in order to obtain these wheat-shaped particles.

### 3.4 Potentiometric titration

The functionalization of the surface can also be studied by potentiometric titration, which gives an indirect evidence of the presence of sulfonic groups. Figure 4 shows the curves corresponding to the titration of the synthesized samples. The resulting acidity strongly depends on the synthesis method used. It can be noticed that the number of acid centers of high acidity is higher when the final functionalization is carried out with chlorosulfonic acid (curve d). Samples SBAsulf1 (curve b) and SBAsulf2 (curve c) have similar level of acidity according to this technique. These results indicate that the acidic groups are stronger when using the chlorosulfonic acid to functionalize the surface (Fuchs et al. 2008).

### 3.5 Catalytic activity

The catalytic activity of functionalized SBA-15 samples in the iso-butane alkylation was investigated to ascertain the acidic properties. The synthesized materials have not shown activity in the alkylation of isobutane with butenes. No reaction products in the C5+ fraction were detected during the

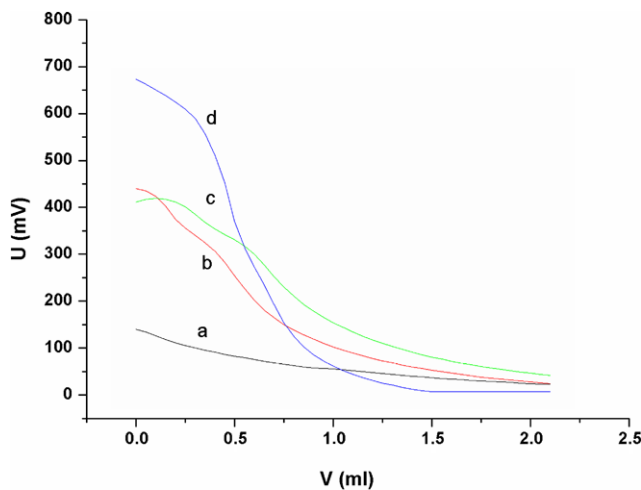
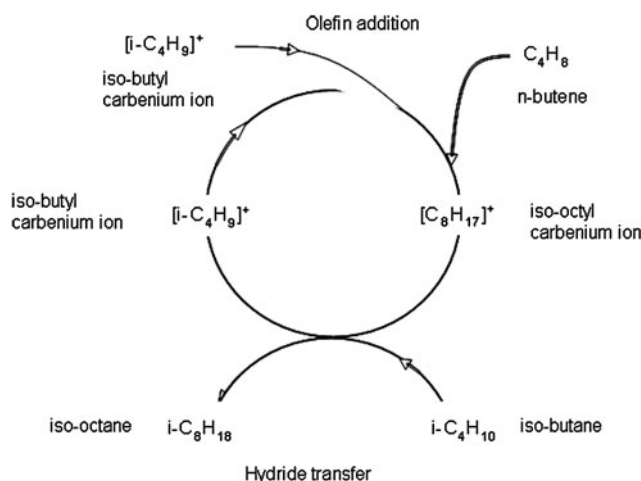


**Fig. 4** Titration with butylamine curves corresponding to sulfonic samples (a) SBAorig, (b) SBAsulf1, (c) SBAsulf2, (d) SBAsulf3



**Scheme 1** Simplified alkylation mechanism

activity test; only the presence of cis and trans 2-butene due to the isomerization of 1-butene. Moreover, the solids discharged from the reactor did not have coke deposits formed during the reaction.

According to the characterization analyses, we can infer that the acidic functionalization of the mesoporous silicas, has been achieved. Then, it is necessary to know whether the adsorption of the olefin on these acid sites actually occurs. This is a fundamental step for the formation of the carbocation responsible for the initiation of the catalytic reaction. Scheme 1 presents a typical reaction mechanism for this reaction. The overall cycle in the alkylation reaction comprises the addition of n-butene to an isobutyl carbenium ion to form an octyl carbenium ion, which in turn is removed from the acid site by hydride transfer from isobutane, leading to trimethylpentanes as primary products and to another isobutyl carbenium ion (Corma and Martinez 1993). Competition between hydride transfer and oligomerization

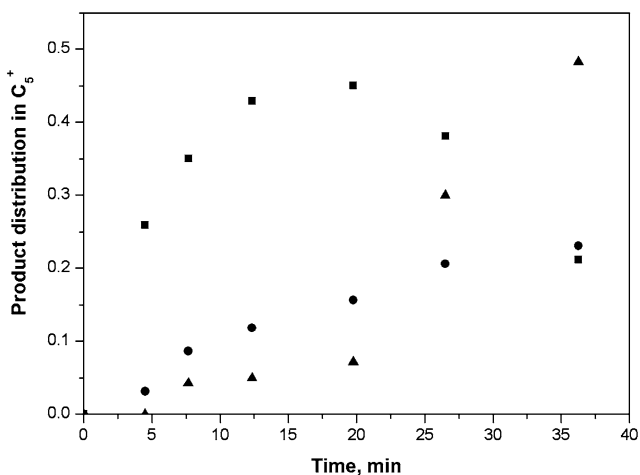


**Fig. 5** Distribution of products Y-LCH (■) TMP, (●) DMH, (▲) DMH=

of butene as secondary reaction determines the lifetime of the catalyst. The higher is the ratio of hydride transfer vs. the rate of oligomerization, the more the primary products trimethylpentanes will be produced and the more the catalyst deactivation will be slowed down (Feller et al. 2003).

Figure 5 shows the distribution of trimethylpentanes (TMP), dimethylhexanes (DMH) and dimethylhexenes (DMH=), in the C5+ fraction (including iso-pentane) obtained in the reaction carried out with the Y-LCH catalyst. Selectivity to TMP (desired products) reaches a maximum value of 50% after approximately 20 min. When the TMP concentration drops, an increase in the DMH= concentration is observed. These compounds are formed by dimerization of butenes and indicate that the catalyst is deactivated for the hydrogen transfer reaction; therefore, mainly dimerization products are obtained. After about 30 min the amount of DMH= becomes more important and the catalyst is completely deactivated. This is because coke deposition on the acid sites causes the reduction of hydrogen transfer activity, which is essential in the alkylation reaction, and changes the catalyst selectivity. On the other hand, the DMH fraction increases gradually along the reaction time.

The density of acid sites of the Y-LCH zeolite as determined by Pyridine TPD (Dalla Costa and Querini 2010) is 1.4 mmoles/g, which correspond to 2.3  $\mu\text{mol}/\text{m}^2$ , being the BET surface for this catalyst 588  $\text{m}^2/\text{g}$ . According to the data presented in the tables shown above, the sample SBAsulf3 that contains 3.32% of sulfur, 670  $\text{m}^2/\text{g}$  and 33% of oxidized sulfur, has a density of active sites of 0.46  $\mu\text{mol}/\text{m}^2$  was obtained. This site density is considerably lower than that for the Y-LCH zeolite and can be a feature related to the lack of activity in the alkylation reaction. The active site density that results for SBAsulf2 and SBAsulf1 are 0.59 and 0.51  $\mu\text{mol}/\text{m}^2$  respectively.

Propylsulfonic SBA-15 has been previously used in the alkylation of isobutane with butenes (Shen et al. 2008). In

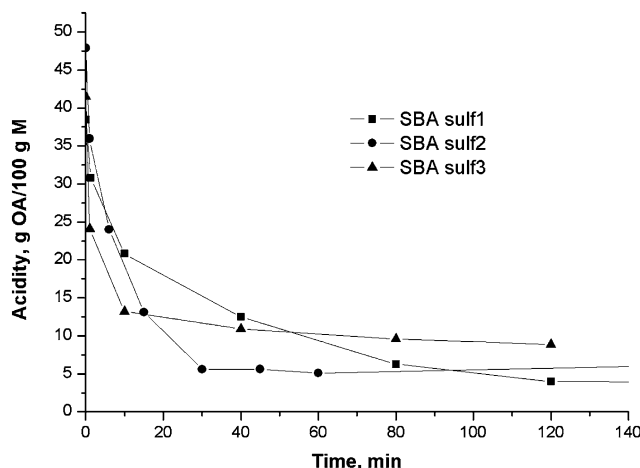


**Fig. 6** Evolution of acidity in the esterification reaction for (a) SBA-Sulf1, (b) SBASulf2, (c) SBASulf3. Initial acidity in the mixture FFA/OIL A° = 40%, Molar Ratio (MR) alcohol/FFA 3:1, catalyst loading 6 wt% referred to the FFA content

this latter publication, a very low activity in this reaction was reported. If 50% of the mercapto groups were oxidized (value not reported), the catalyst they used had an acid site density of  $0.26 \mu\text{mol}/\text{m}^2$ , which is approximately half of the density we obtained in this work.

On the other hand, when the catalysts were tested in the reaction of esterification of FFA with methanol they showed activity. Figure 6a shows the Acidity (A) as a function of time during the esterification with the samples SBASulf1 (a), SBASulf2 (b) and SBASulf3 (c). In all cases, a high initial reaction rate is observed, noticing that the sample SBASulf3 is the better. However, this catalyst produces the lowest conversion, reaching a final value of 78.7% after 2 h of reaction (see Fig. 6b). Using the data shown in Fig. 6a, it is possible to estimate the initial reaction rate, in the case of the esterification reaction. It can be clearly seen that the initial reaction rate is higher in the case of the sample SBASulf3, which was treated with chlorosulfonic acid, being  $0.013 \text{ mol}/(\text{L}\cdot\text{s})$ , and  $0.008$  and  $0.004 \text{ mol}/(\text{L}\cdot\text{s})$  in the case of the SBASulf2 and SBASulf1 respectively. The potentiometric results shown above, also indicates that the sample SBASulf3 has the strongest acid sites, while the other two functionalized samples display similar values. On the other hand, as previously presented, the acid site density follows the order: SBASulf2 > SBASulf3 > SBASulf1. Consequently, these results demonstrate that in this catalysts series, the more important physicochemical parameter that determines the esterification reaction rate, is the acid site strength, at least within the acid site density displayed by these materials ( $0.46$  to  $0.59 \mu\text{mol}/\text{m}^2$ ).

The sample SBASulf2 shows a higher conversion, being at low reaction times (30 min) 89.3%, while the SBASulf3 reaches a similar conversion (89.7%) but at longer times, i.e., with a lower reaction rate.

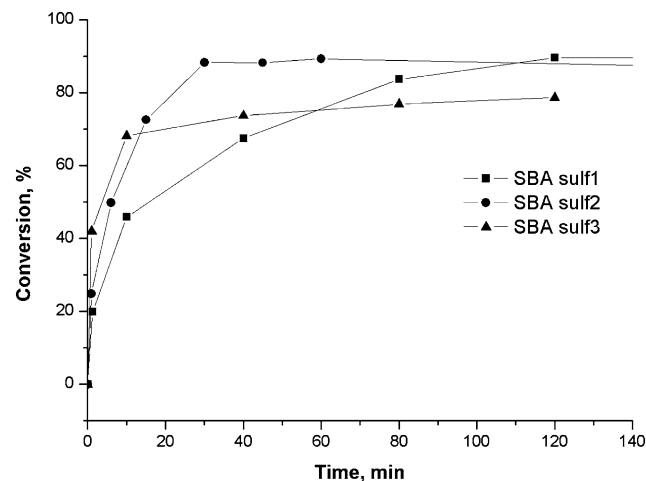


**Fig. 7** FFA conversion for (a) SBASulf1, (b) SBASulf2, (c) SBASulf3

According to the results of potentiometric titration, it can be noticed that a stronger acid catalyst has a higher reaction rate of esterification. However, it is interesting to note that the final value is different among the three catalysts, what suggest that the catalysts deactivates at different rate.

The fact that these materials are active for this reaction indicates that they have strong acidity. Therefore, the lack of activity for the alkylation reaction is not related to low catalyst acidity, but is determined by other factors that prevent the reaction occurrence. There are two main possible reasons for this behavior. One of them is that the site density requirement is different for both reactions, being higher for the alkylation, and the catalysts used in this study have not enough acid sites to reach this density. The other reason is that the surface is hydrophilic, and consequently the butenes and isobutane can not be activated on the surface, while free fatty acids and methanol are activated. This latter explanation agrees with the results reported by Shen et al. (2010). They found that by modifying the hydrophilic character of the surface, getting a hydrophobic support, a better catalyst for isobutane alkylation is obtained. It has to be emphasized, that these catalysts are active for fatty acid esterification but inactive for isobutane alkylation, which are two reactions carried out at industrial levels with the same catalyst, i.e. sulphuric acid.

### 3.6 1-butene pulses experiments

Figure 7 shows the signal obtained in the blank experiment, carried out with an empty cell. The experiments performed with the synthesized materials are compared with this blank. When an interaction between the catalyst and the olefin occurs, a reduction of amplitude and a modulation of the signal are observed.

Pulses of 1-butene were consecutively sent to the catalyst sample at different temperatures, both while going from low

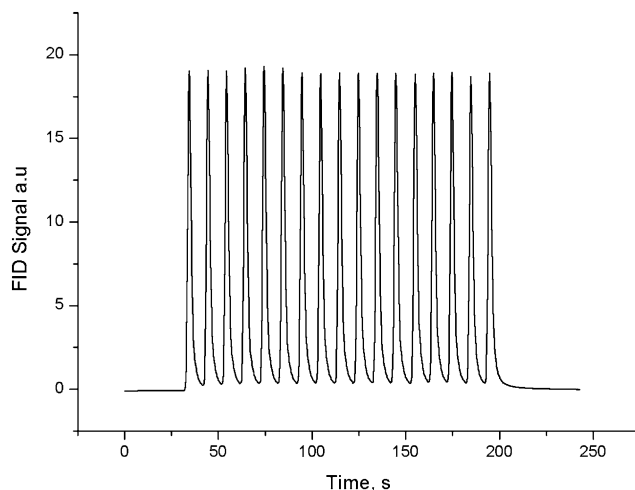


**Fig. 8** Pulses of 1-butene empty cell, blank

temperature (e.g. 60 °C) up to high temperature (100 °C), and then when the temperature was decreased, in steps of 10 °C. Pulse experiments for the Y-LCH catalyst and comparisons with catalysts from Beta zeolite were reported in a previous work. Figure 8a shows the signal obtained with the Y-LCH catalyst at 60 °C. It can be noticed that after approximately 200 seconds (20 pulses) the average amount of butene coming out of the cell is equal to the injected amount. At the beginning of this pulse series, a transient zone, in which the average value is clearly lower than the input amount, can be observed. Therefore, this type of signal indicates that certain amount of butene is being irreversibly adsorbed on the catalyst. The small and constant amplitude observed in the reversible zone indicates that one or both of the two following processes are taking place: (a) diffusion in and out of the micropore system; (b) adsorption and desorption in a pseudo steady state. In both cases, all butene that was injected comes out of the cell. If butene is irreversibly adsorbed, it will cause a decrease in the number of adsorption sites. As a result, the oscillation amplitude should increase as the number of pulses increases. If the mean value of the signal is lower than that corresponding to the blank, then the butene is being irreversibly adsorbed on the catalyst. At 60 °C, the first series of pulses (full line) and the last one (dotted line) after all the pulses at increasing and decreasing temperatures have been sent, are almost equal, and of small amplitude. This indicates that the catalyst suffers small changes in its adsorption capacity, and that there is no pore mouth plugging. If pore mouth plugging occurs, the amplitude must be equal to that observed in the blank experiment, since no diffusion in and out of the pores, or adsorption-desorption can take place and, therefore, the signal should not be modulated.

Figure 8b shows that at 80 °C, the adsorption-oligomerization process is faster than at 60 °C. A stronger signal is

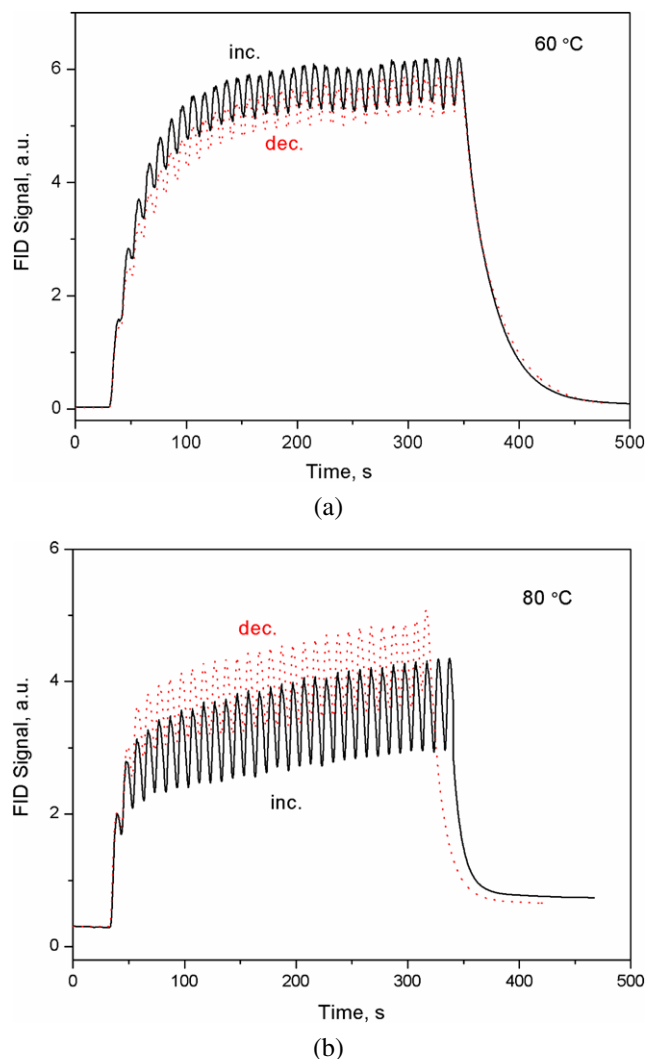


**Fig. 9** (a) Pulses of 1-butene at 60 °C, Y-LCH. (b) Pulses of 1-butene at 80 °C, Y-LCH; *inc.*: pulses sent during the first part of the experiment, increasing the temperature in 10 °C steps; *dec.*: pulses sent while decreasing the temperature in 10 °C steps

observed for the deactivated catalysts (dotted line) as compared to the response obtained during the temperature increase (full line). This indicates that a fraction of butene fed during the consecutive pulses sent along this experiment is deposited on the catalyst, leading to an adsorption capacity loss. However, the difference between these two signals is not very large, so we can conclude that this phenomenon is not very important. The amount of coke measured after the pulse experiment was 5.37%.

In the case of the functionalized mesoporous silicas, no interaction with butene was observed when conducting pulse experiments. At 60 and 80 °C the response obtained for both SBA-sulf2 and SBA-sulf3 samples is similar to that for the blank. Figure 9 shows the results obtained with sample SBA-sulf3. Similar results were obtained for sample SBA-sulf2 and SBA-sulf1. After the pulse experiments, these samples

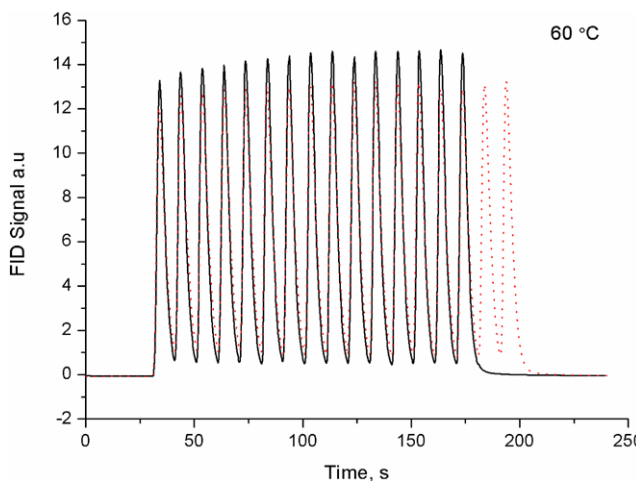


**Fig. 10** Pulses of 1-butene at different temperatures for SBAsulf3

did not show the presence of coke, indicating that no butene adsorption has occurred. Therefore, the inactivity of these mesoporous catalysts may be because the propyl-sulfonic groups anchored to the surface are not able to form and stabilize the carbocation from the olefin. Consequently the reaction mechanism cannot start.

These experiments were performed in gas phase, while the activity test was carried out in liquid phase. However, a qualitative analysis of the interaction between the olefin and the catalyst surface can be done. Those catalysts that show no interaction in gas phase will probably not interact in the liquid phase. According to our studies with a large variety of acid catalysts, there is a correlation, at least for this reaction, between the activity for isobutane alkylation and the interaction of the catalyst surface with butenes in gas phase.

#### 4 Conclusions

Solid acid catalysts were synthesized by anchoring sulfonic groups on mesoporous silica SBA-15 surface, using different functionalization methodologies. The XPS, FTIR, and potentiometric titration techniques showed an effective incorporation of sulfonic groups, regardless of the synthesis procedure employed. However, when generation of sulfonic groups is based on oxidation of the mercapto groups, the generated catalyst has an acid strength lower than that achieved when the sulfonic groups are incorporated in a direct form on pre-attached mercapto groups. These acid catalysts did not show activity for the alkylation of isobutane with C4 olefins, behavior which was correlated with the results of dynamic adsorption of butene, but they showed activity in the FFA esterification. The lack of activity of these materials in the isobutane alkylation can be due to the fact that propylsulfonic groups anchored onto the surface do not

interact properly with the olefin molecule to achieve the formation and stabilization of the carbocation species required to initiate the reaction. This may be due to the polar environment in the pores of these catalysts, which is not suitable for adsorption of the olefin.

**Acknowledgements** The authors would like to thank UTN for financial support. M.S.L. acknowledges the grant for her Ph.D. study sponsored by FONCyT/UTN.

#### References

- Bossaert, W.D., De Vos, D.E., Van Rhijn, W.M., Bullen, J., Grobet, P.J., Jacobs, P.A.: Mesoporous sulfonic acids as selective catalysts for synthesis of monoglycerides. *J. Catal.* **182**, 156–164 (1999)
- Bulut, M., Erk, C.: Improved synthesis of some hydroxycoumarins. *Dyes Pigm.* **30**, 99–104 (1996)
- Chakrabarti, A., Sharma, M.M.: Cationic ion exchange resins as catalysts. *React. Polym.* **20**, 1–45 (1993)
- Corma, A., Martinez, A.: *Catal. Rev. Sci. Eng.* **35**, 483 (1993)
- Dalla Costa, B.O., Querini, C.A.: Isobutane alkylation with solid catalysts based on beta zeolite. *Appl. Catal. A, Gen.* **385**, 144–152 (2010)
- Dalla Costa, B.O., Tara, J.C., Basaldella, E.I., Querini, C.A.: Alquilación de isobutanos con 1-buteno. Desarrollo de nuevos catalizadores. In: *Actas del XVI Congreso Argentino de Catálisis* (CD-ROM), Buenos Aires, Argentina (2009)
- Feller, A., Barth, J.-O., Guzman, A., Zuazo, I., Lercher, J.A.: *J. Catal.* **220**, 192 (2003)
- Ford, D.M., Simanek, E.E., Shantz, D.F.: Ordered mesoporous silica as model substrates for building complex hybrid materials. *Nanotechnology* **16**, 458–475 (2005)
- Fuchs, V.M., Pizzio, L.R., Blanco, M.N.: Hybrid materials based on aluminum tungstophosphate or tungstosilicate as catalysts in anisole acylation. *Catal. Today* **133–135**, 181–186 (2008)
- Ginosar, D.M., Thompson, D.N., Burch, K.C.: Recovery of alkylation activity in deactivated USY catalysts using supercritical fluids: a comparison of light hydrocarbons. *Appl. Catal. A, Gen.* **262**, 223–231 (2004)
- Hamoudi, S., Kaliaguine, S.: *Microporous Mesoporous Mater.* **59**, 195 (2003)
- Hamoudi, S., Royer, S., Kaliaguine, S.: *Microporous Mesoporous Mater.* **71**, 17 (2004)
- Harmer, M.A., Sun, Q.: Solid acid catalysis using ion-exchange resins. *Appl. Catal. A, Gen.* **221**, 45–62 (2001)
- Izumi, Y., Urabe, K., Onaka, M.: *Zeolite, Clay and Heteropoly Acid in Organic Reactions*. Weinheim, New York (1993)
- Kozhevnikov, M.I.V.: *Catalysis by Polyoxometalates*. Wiley, Chichester (2002)
- Li, N., Li, X., Wang, W., Geng, W., Qiu, S.: Blue-shifting photoluminescence of Tris (8-hydroxyquinoline) aluminium encapsulated in the channel of functionalized mesoporous silica SBA-15. *Mater. Chem. Phys.* **100**, 128–131 (2006)
- Lim, M.H., Stein, A.: Comparative studies of grafting and direct syntheses of inorganic-organic hybrid mesoporous materials. *Chem. Mater.* **11**, 3285–3295 (1999)
- Margolese, D., Melero, J.A., Christiansen, S.C., Chmelka, B.F., Stucky, G.D.: Direct synthesis of ordered SBA-15 mesoporous silica containing sulfonic acid groups. *Chem. Mater.* **12**, 2448–2459 (2000)
- Melero, J.A., Grieken, R.V., Morales, G.: *Chem. Rev.* **106**, 3790 (2006)

Moffat, J.B.: Metal-Oxygen Clusters. The Surface and Catalytic Properties of Heteropoly Oxometalates. Kluwer/Academic, New York (2001)

Niknam, K., Saberi, D., Sefat, M.N.: Silica-bonded S-sulfonic acid as a recyclable catalyst for chemoselective synthesis of 1,1-diacetates. *Tetrahedron Lett.* **50**, 4058–4062 (2009)

Olah, G.A., Prakash, G.K.S., Sommer, J.: Superacids. Wiley, New York (1985)

Phan, N.T.S., Jones, C.V.: Highly accessible catalytic sites on recyclable organosilane-functionalized magnetic nanoparticles: an alternative to functionalized porous silica catalysts. *J. Mol. Catal. A, Chem.* **253**, 123–131 (2006)

Potdar, M.K., Mohile, S.S., Salunkhe, M.M.: Coumarin synthesis via Pechman condensation in Lewis acidic chloroaluminate ionic liquid. *Tetrahedron Lett.* **42**, 9285–9287 (2001)

Querini, C.A., Roa, E.: Deactivation of solid acid catalysts during isobutane alkylation with C4 olefins. *Appl. Catal. A, Gen.* **163**, 199–215 (1997)

Querini, C.A., Roa, E., Pieck, C.L., Parera, J.M.: Isobutane alkylation with C4 olefins: low temperature regeneration of solid acid catalysts with ozone. *Stud. Surf. Sci. Catal.* **111**, 407–414 (1997)

Robertson, A., Sandrock, W.F., Henery, C.B.: Hydroxy-carbonyl compounds. Part V. The preparation of coumarins and 1: 4-pyrones from phenol, *p*-cresol, quinol, and  $\alpha$ -naphthol. *J. Chem. Soc.* 2426–2432 (1931)

Russell, A., Frye, J.R.: Organic Syntheses. Wiley, New York (1955)

Sharma, M.M.: Some novel aspect of cationic-exchange resins as catalysts. *Funct. Polym.* **26**, 3–23 (1995)

Shen, W., Dubé, D., Kaliaguine, S.: *Catal. Commun.* **10**, 291–294 (2008)

Shen, W., Gua, Y., Xu, H., Dube, D., Kaliaguine, S.: *Appl. Catal. A, Gen.* **377**, 1–8 (2010)

Sing, K.S.W., Everett, D.H., Haul, R.A.W., Moscou, L., Pierotti, R.A., Rouquerol, J., Siemieniewska, T.: Reporting physisorption data for gas/solid systems with special reference to the determination of surface area and porosity. *Pure Appl. Chem.* **57**, 603–619 (1985)

UNE-EN 14104: Determination of acid value (2003)

Wight, A.P., Davis, M.E.: Design and preparation of organic-inorganic hybrid catalysts. *Chem. Rev.* **102**, 3589–3614 (2002)

Yang, C.T., Huang, M.H.: Formation of arrays of gallium nitride nanorods within mesoporous silica SBA-15. *Phys. Chem. B* **109**, 17842–17847 (2005)

Yoshitake, H.: Highly controlled synthesis of organic layers on mesoporous silica: their structure and application to toxic ion adsorption. *J. Chem.* **29**, 1107–1117 (2005)

Zhao, D., Huo, Q., Feng, J., Chmelka, B.H., Stucky, G.D.: Nonionic triblock and star diblock copolymer and oligomeric surfactant synthesis of highly ordered, hydrothermally stable, mesoporous silica structures. *J. Am. Chem. Soc.* **120**, 6024–6036 (1998)